

Determination of structures of complexes in solution from X-ray diffraction data

Georg Johansson

Department of Inorganic Chemistry, Royal Institute of Technology,
S-100 44 Stockholm, Sweden.

Abstract - Methods for deriving structures of complexes in solution from X-ray diffraction data are discussed. The use of isomorphous substitution for separating specific interactions is demonstrated for some systems with inner- and outer-sphere complex formation. The results are used to illustrate the difficulties encountered in making unique interpretations of solution diffraction data.

INTRODUCTION

Knowledge of structures of complexes in solution is fundamental for interpretation of thermodynamic and kinetic data, but detailed information on coordination numbers and intramolecular distances is not usually available. For complexes occurring in both the solid state and solution, the solid state bond distances are generally assumed to be valid also in solution, although they are likely to be affected by the solvent used and by differences in concentration and counter ions. Many complexes exist only in solution and are not known from crystal structure determinations.

The only methods available, which can give direct structural information in terms of interatomic distances and bond angles, are based on diffraction. The liquid state, however, is not very favorable for a structure determination by means of diffraction methods. It does not have the three-dimensional order which for a crystal gives a structure which can be fully described by a limited number of parameters and leads to a strong three-dimensional diffraction pattern. Also for a gas, conditions are more favorable since its one-dimensional diffraction pattern results from intramolecular interactions only, which are directly related to the structure of the individual gas molecule. For a solution the diffraction effects are weak and since the molecules are closely packed, intramolecular as well as intermolecular interactions will contribute to the diffraction and will complicate the derivation of the structures.

The limitations inherent in conventional X-ray diffraction studies are partially overcome by EXAFS methods (extended X-ray absorption fine structure) (ref. 1) and the use of differential anomalous scattering (ref. 2), which can give information on the environment around specific atoms in a solution. Both, however, require the use of synchrotron radiation, which is not generally available, and they have limitations of their own. EXAFS sometimes seems to give uncertain coordination numbers as well as distances. The anomalous scattering method depends on relatively small differences in scattering powers and has not yet been extensively used. Even in conventional diffraction methods a separation of interactions involving specific atoms can sometimes be made. In neutron diffraction this can be accomplished by using isotopic substitution (ref. 3), when suitable isotopes are available. In X-ray diffraction a similar result can be achieved by using isomorphous substitution (ref. 4).

In a crystal structure determination, based on diffraction data, the number of independent experimental observations exceeds the number of parameters to be determined. The system is overdetermined and a unique structure determination is almost always possible. For a non-ordered state, the number of parameters needed to describe the structure is not limited, as for a crystal, and only a one-dimensional diffraction curve is usually available for the determination of an essentially three-dimensional structure. The system is underdetermined and a structural model, consistent with the scattering data, will not necessarily be unique and may not exclude the possible existence of other models, which may give equal or better agreement. An overinterpretation of the data can easily be made. A structural model, on the other hand, which is not consistent with the scattering data, can be excluded.

An increasing number of diffraction investigations of liquids and solutions are being carried out but relatively few of these have involved structure determinations of complexes. The major interest seems to have been concentrated on hydrated metal ions in aqueous solution, primarily as part of investigations on structures of electrolyte solutions. Consequently, ions from the first two groups in the periodic system have been the subject of a large number of investigations (ref. 5-10).

The structure of a solvated ion and the structural change caused by the replacement of a solvent molecule in the coordination sphere by a mono or polydentate ligand can in principle be determined by diffraction methods. The stepwise building up of metal-ligand complexes from the solvated metal ion can involve several coordination changes in addition to changes in bond lengths and bond angles. Direct information on the structures of inner and outer sphere complexes can be obtained by following changes in the diffraction patterns over a range of concentrations. Polynuclear complexes often formed in solution, for example in hydrolysis reactions, can be profitably studied by diffraction methods because of the distinct metal-metal interactions in the complexes. Another interesting field is that of very concentrated electrolyte solutions. The structural change taking place when a metal ion hydrate melts can be followed by diffraction measurements and can be related to its crystal structure. The molten hydrate provides a link between the crystal structure and the very concentrated electrolyte solutions, where the ordering is more pronounced than in dilute solutions and for which the structures are not well known.

Direct structural information on complexes formed in solution is needed and diffraction measurements can provide at least part of this information. The results cannot be compared to those from a crystal structure determination, but are in many cases, when combined with information from other sources, sufficient for a derivation of the structures.

TREATMENT OF DATA

Experimental

Usually the intensity of the radiation scattered from the free surface of the solution is measured as a function of the scattering angle, 2θ , in an arrangement having the Bragg-Brentano parafocusing geometry (Fig. 1). The scattered radiation is filtered through a focusing single crystal lithium fluoride monochromator. Graphite can be used but is less efficient in reducing unwanted radiation. The measured intensities are corrected for background, absorption, multiple scattering and incoherently scattered radiation.

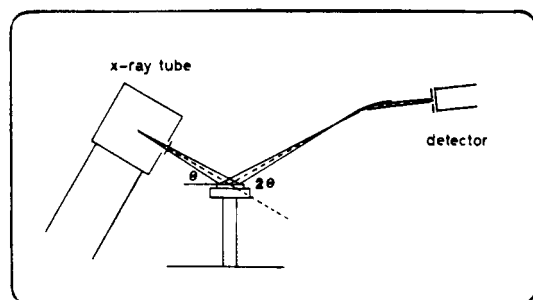


Fig. 1. Experimental arrangement for X-ray diffraction measurement on solutions.

Theoretical

For a solution the structure can be described by correlation functions, $g_{pq}(r)$, which give the time averaged probability of finding an atom "q" at a distance r from an atom "p". The number of "q" atoms between two spherical shells of radii r_1 and r_2 surrounding a "p" atom is then given by the expression:

$$n = n_q V^{-1} 4\pi \int_{r_1}^{r_2} r^2 g_{pq}(r) dr \quad (1)$$

where $n_q V^{-1}$ is the number of atoms "q" in a unit volume V . By a Fourier transformation of the correlation function the partial structure factor, $S_{pq}(s)$, is obtained:

$$S_{pq}(s) = 1 + 4\pi N V^{-1} s^{-1} \int (g_{pq}(r) - 1) \cdot r \cdot \sin(rs) \cdot dr \quad (2)$$

Here $s = 4\pi\lambda^{-1} \sin\theta$. The wave length of the radiation is λ and the scattering angle is 2θ . N is the total number of particles in the volume V .

If the partial structure factor has been determined the corresponding correlation function can be calculated by a Fourier transformation:

$$g_{pq}(r) = 1 + V(2\pi^2Nr)^{-1} \int (S_{pq}(s)-1) \cdot s \cdot \sin(rs) \cdot ds \quad (3)$$

If a solution contains n different atomic species the number of different partial structure factors is $n(n+1)/2$. The total structure factor is obtained as a sum over the partial structure factors and the total correlation function is the sum over the corresponding partial correlation functions.

The total scattered intensity from a solution, measured as a function of s in an X-ray diffraction experiment and normalized to a unit volume, is equal to

$$I(s) = \sum_p n_p f_p^2 + \sum_p \sum_q n_p n_q f_p(s) f_q(s) (S_{pq}(s)-1) \quad (4)$$

where $f(s)$ are the X-ray scattering factors for the atoms. The structure factors, $S(s)$, approach unity for large values of s which can be used for a normalization of the observed intensities to a unit of volume chosen, by comparing observed intensities at large scattering angles with the independent coherent scattering $\sum_p n_p f_p^2$. By subtracting the term $\sum_p n_p f_p^2$ from the normalized intensity values the structure dependent part, the reduced intensity function $i(s)$, remains:

$$i(s) = I(s) - \sum_p n_p f_p^2 = \sum_p \sum_q n_p n_q f_p(s) f_q(s) (S_{pq}(s)-1) \quad (5)$$

Since the X-ray scattering factors, $f(s)$, are functions of s the measured intensities are not linear combinations of the different partial structure factors and a Fourier transformation results in a convoluted correlation function. Since the contributions to $i(s)$ are weighted by the product of the scattering factors, and these depend on the number of electrons in an atom, light atoms contribute much less than heavy atoms.

An electronic radial distribution function, $D(r)$, can be calculated from the observed $i(s)$ values and is defined by the expression:

$$D(r) = 4\pi r^2 \rho_0 + 2\pi r^{-1} \int s \cdot i(s) \cdot M(s) \cdot \sin(rs) \cdot ds \quad (6)$$

where $\rho_0 = (\sum_p n_p Z_p)^2 / V$ and $\sum_p (n_p Z_p)$ is the total number of electrons in the unit volume. $M(s)$ is a sharpening function introduced to compensate for the decrease in the values of the scattering factors when s increases.

The radial distribution function, $D(r)$, is a sum over the convoluted partial radial distribution functions and this makes its information contents rather limited. For a complex in a solution the interactions of interest are those involving the complex forming ions and a separation of the corresponding interactions is needed for a determination of its structure. Two methods are available which can achieve this. Isomorphic substitution leads to a separation of the partial distribution functions involving the substituted ion, but its use is limited by the number of available isomorphous pairs. The specific characteristics of intramolecular interactions can be used to separate them from those of other interactions in the solution.

Isomorphic substitution

An aqueous solution of a metal salt, ML_p , contains four different atomic species: the metal ion "M", the ligand "L", and the atoms of the water molecules "O" and "H". The total number of partial distribution functions is ten. If the number of atoms of each type in the unit volume is given by n_M , n_L , n_O and n_H , respectively, we can write

$$\begin{aligned} i(s) = & 2n_M n_O f_M f_O [S_{MO}(s)-1] + 2n_M n_L f_M f_L [S_{ML}(s)-1] + 2n_M n_H f_M f_H [S_{MH}(s)-1] + \\ & n_M^2 f_M^2 [S_{MM}(s)-1] + n_O^2 f_O^2 [S_{OO}(s)-1] + 2n_O n_L f_O f_L [S_{OL}(s)-1] + \\ & 2n_O n_H f_O f_H [S_{OH}(s)-1] + n_L^2 f_L^2 [S_{LL}(s)-1] + 2n_L n_H f_L f_H [S_{LH}(s)-1] + \\ & n_H^2 f_H^2 [S_{HH}(s)-1] \end{aligned} \quad (7)$$

The parts of this expression characterizing the metal ion interactions can be separated if a substituent ion M' can be found, which has a scattering power differing from that of M , but does not change the structure of the solution when replacing M . The difference between

observed intensities for two solutions of the same compositions, one containing M and the other M', will then contain only terms involving the metal ion, other terms being unchanged:

$$\Delta i(s) = 2n_M n_O f_O \Delta f_M [S_{MO}(s)-1] + 2n_M n_L f_L \Delta f_M [S_{ML}(s)-1] + 2n_M n_H f_H \Delta f_M [S_{MH}(s)-1] + n_M^2 (f_{M2} - f_M \cdot 2) [S_{MM}(s)-1] \quad (8)$$

where $\Delta f_M = f_M - f_{M'}$. Normally the first two terms will be much larger than those involving MH and MM interactions. A Fourier transformation using the convolution function $f_M/\Delta f_M$ deconvolutes these terms in the difference function:

$$D^M(r) = 4\pi r^2 \rho_M + 2r\pi^{-1} \int s \cdot \Delta i(s) \cdot \sin(rs) \cdot M(s) \cdot f_M (\Delta f_M)^{-1} \cdot ds \quad (9)$$

where $\rho_M = (\sum n_i Z_i)^2/V$ includes only terms involving the metal ion and $D^M(r)$ is the part of the distribution function that involves the metal ion interactions.

A difference in bonding distances between M and M' would require a correction term in this expression. In the examples, which will be discussed in the following, the differences are small (≈ 0.01 Å) and the correction term will be ignored. It will also be assumed that for the solutions and for the range of distances discussed the M-M interactions are not important.

Intra- and intermolecular interactions

For sharp interactions between two atoms "p" and "q", resulting from well defined intramolecular distances, the contribution to the intensity curve can be calculated from the Debye expression

$$i(s) = 2\sum f_p f_q \cdot (r_{pq})^{-1} \sin(r_{pq} s) \cdot \exp(-\frac{1}{2} l_{pq}^2 s^2) \quad (10)$$

This is valid if each distance, r_{pq} , has a gaussian distribution about its average with a root mean square variation of l_{pq} Å. A sharp interaction, having a small l_{pq} value, will give larger contributions to the intensity curve at higher s values than that of an interaction with a larger l_{pq} . Well-defined distances will, therefore, be dominant contributors to the high-angle part of a diffraction curve while other distances and non-bonded interactions will contribute only in the low-angle region of the curve. The corresponding contribution to the D(r) function can be obtained by a Fourier transformation analogous to the one used for the experimental i(s) values. An intramolecular interaction will lead to a distinct peak in the RDF, which can usually be distinguished from the diffuse peaks resulting from distances between non-bonded atoms.

The scattering data can thus be analyzed in s space, by comparing observed and theoretical i(s) values, or in r space, by comparing calculated peaks with those observed in the RDF. In r space the intermolecular interactions are broad and diffuse. In s space they fade out quickly. The intramolecular interactions, on the other hand, cause significant oscillations in the structure factor even at high s values and result in sharp peaks in the RDFs.

STRONG COMPLEXES DOMINATING THE SCATTERING

Under favorable conditions an analysis of a single diffraction curve can lead to a unique and precise structure determination of a dissolved complex. The procedure can be illustrated by an investigation of the square planar $PtCl_4^{2-}$ complex, for which concentrated aqueous solutions can be prepared in which it is the only dominant complex (ref. 11).

For a 1 M $(NH_4)_2PtCl_4$ solution the experimental data are illustrated in Fig. 2a. The structure dependent part of the scattered intensity appears as oscillations around the smoothly decreasing background curve of the independent coherent scattering $\sum n_p f_p^2$. If this is subtracted the reduced intensity curve, i(s), is obtained which contains the structural information on the solution and forms the basis for the analysis (Fig. 2b). A Fourier transformation converts the data from s space to r space and gives the radial distribution function (Fig. 2c). The three intramolecular distances in the square planar $PtCl_4^{2-}$ complex lead to distinct peaks in the RDF. By comparison with theoretical Pt-Cl and Cl-Cl peaks the relative frequency of each peak can be approximately estimated, which, together with the ratios between the observed distances (Pt-Cl:Cl-Cl:Cl-Cl = (1 : $\sqrt{2}$: 2)), uniquely determine the structure of the square planar complex. Calculated values for the intramolecular contributions to the reduced intensity curve reproduce the experimental curve closely, except in the low-angle region, where they no longer dominate over intermolecular interactions in the solution (Fig. 2b). Subtracting calculated values from observed values leaves very little of remaining structure in the diffraction curves, because of the dominant contribu-

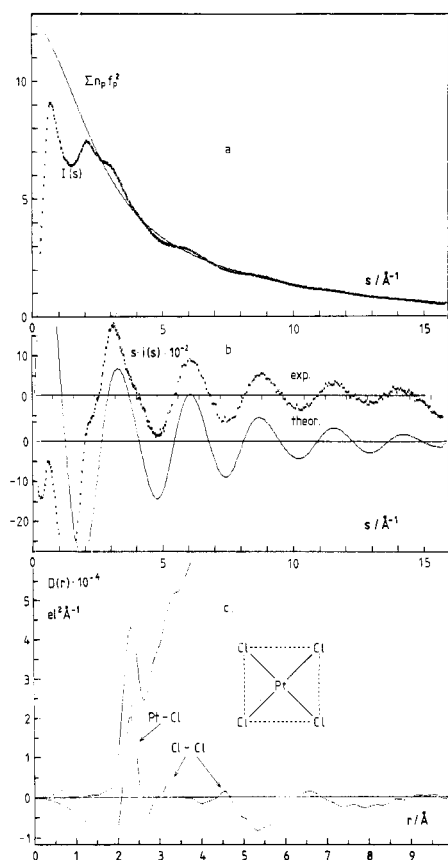


Fig. 2. Results of diffraction measurements on a 1 M $(\text{NH}_4)_2\text{PtCl}_4$ solution: Normalized observed intensities and independent coherent scattering (a), observed and calculated $s \cdot i(s)$ values (b) and $D(r)$ and $D(r) - 4\pi r^2 \rho_0$ functions (c).

tions from the heavy metal complex. The region of the intensity curve in which the intramolecular interactions dominate over all other interactions in the solution is sufficiently large to make a least squares refinement possible for the parameters characterizing them, that is distance, d , frequency, n , and rms variation, l .

The Pt-Cl distances can be determined with an accuracy equal to or better than in a corresponding crystal structure determination, since data are available up to large θ values. Because of strong correlation between frequency and rms variation the accuracy with which these parameter values can be determined will depend on the size of the s range in which the interaction is dominant.

The Pt-Cl distance can be determined also from the peak position in the RDF. The peak size and shape should give the frequency of the distance and its rms variation, but since the Pt-Cl peak is partly overlapped by neighboring peaks (Fig. 2c) a further separation of interactions is needed in order to get more precise information. The tetrachloro complex of palladium(II) has the same square planar structure as PtCl_4^{2-} . According to crystal structure determinations the Pt-Cl and the Pd-Cl bond lengths are equal and this is confirmed for solutions by diffraction measurements. Palladium can, therefore, be used as an isomorphous substituent for Pt and a separation of interactions can be made. The result of the separation is shown in Fig. 3. The Pt-Cl peak is now fully resolved and can be closely reproduced by a theoretical peak calculated for 4 Pt-Cl distances of 2.311 Å with an rms variation of 0.063 Å. The longer interactions in which the Pt atom is involved begin to emerge at about 3 Å, but do not indicate any pronounced structure around the PtCl_4^{2-} complex (Fig. 3a). The non-metal interactions in this region are dominated by $\text{H}_2\text{O}-\text{H}_2\text{O}$ and $\text{Cl}-\text{H}_2\text{O}$ interactions (Fig. 3b).

The results demonstrate that intramolecular interactions can be closely described by Gaussian peaks and can be analyzed by comparison with theoretical peaks calculated according to the Debye expression. This makes a quantitative analysis of a peak possible even if it is not fully resolved in an RDF.

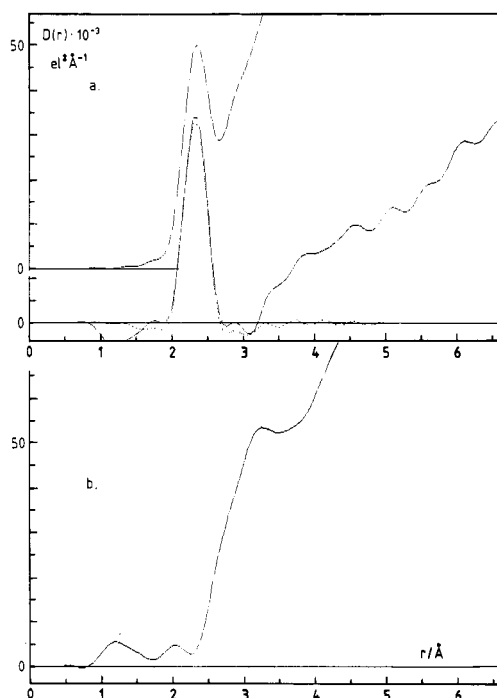


Fig. 3. $D(r)$ and $D^M(r)$ functions for 1 M $(\text{NH}_4)_2\text{PtCl}_4$. The dotted line is a theoretical Pt-Cl peak with $d=2.31$ Å, $n=4.0$, $l=0.063$ Å (a). The part of $D(r)$ not involving Pt (b.).

INNER- AND OUTER-SPHERE COMPLEX FORMATION

Inner sphere complex formation takes place when water molecules in the 1st coordination sphere of the metal ion are replaced by ligands. When the corresponding metal-ligand distances differ from the metal-water bonding distances and occur below the water-water interactions in the bulk water the corresponding peaks are at least partly resolved and can be approximately analyzed in terms of distance, frequency and rms variation for the interactions. Outer-sphere complexes are formed when ligands replace solvent molecules in the 2nd coordination sphere. The corresponding metal-solvent and metal-ligand distances will be longer and will occur in a region where a large number of other distances in the solution will also appear. A quantitative analysis will then not usually be possible.

The effects of complex formation on a diffraction curve is best demonstrated with a system where isomorphous substitution can be used for a separation of interactions. The three-valent ions within the lanthanide series are suitable examples since an isomorphous pair is available among them (ref. 12). They interact primarily electrostatically and their complex formation in aqueous solution is weak. Yttrium, which chemically is closely related to the lanthanides, has an ionic radius of the same magnitude as the lanthanides close to erbium in the series. Yttrium and erbium form apparently isostructural solutions which can be used to study the first and second coordination spheres around the metal ions and the effects of different counter ions and concentrations.

Results for 1 M and 3 M aqueous solutions of erbium perchlorate are given in Fig. 4. In their RDFs (Figs. 4a) the intramolecular interactions in ClO_4^- give peaks at about 1.5 Å (Cl-O) and 2.4 Å (O-O). Er-H₂O interactions in a 1st coordination sphere are expected at about 2.4 Å. The Cl-O peak is resolved in the $D(r)$ function and can be analyzed by comparison with theoretical peaks. The Er-H₂O peak is best resolved in the concentrated solution, where bulk water interactions at about 2.9 Å are less frequent. Approximate parameter values can be obtained by comparison with theoretical peaks.

In the separated RDFs (Figs. 4b) the Er-H₂O peak is fully resolved for both solutions and is closely reproduced by a theoretical peak calculated for a coordination number of 8.0 and a distance of 2.36 Å with an rms variation of 0.10 Å. A 2nd coordination sphere is indicated at 4.5 Å and is in approximate agreement with a gaussian peak for $d = 4.50$ Å, $n \approx 13$ and $l = 0.24$ Å. The ClO_4^- interactions appear in the non-erbium part of the RDFs (Figs. 4c). The Cl-O peak is consistent with a calculated peak for a Cl-O distance of 1.46₅ Å with a rms value of 0.030 Å. The O-O peak is partly resolved only in the concentrated solution.

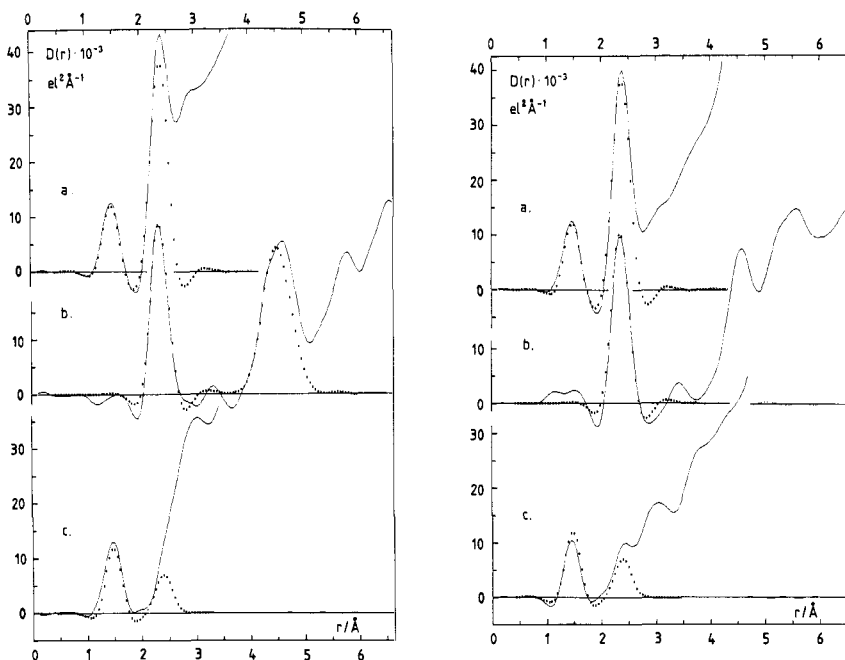


Fig. 4. Radial distribution functions for a 1.00 M (left) and a 2.88 M (right) erbium perchlorate solution. Both data sets normalized to a unit volume containing one Er atom. Dotted lines are theoretical peaks calculated for Cl-O in ClO_4^- : $d=1.465$ Å, $n=4.0$, $l=0.030$ Å.

Er-H₂O in 1st coord. sphere: $d=2.36$ Å, $n=8.0$, $l=0.10$ Å

Er-H₂O in 2nd coord. sphere: $d=4.50$ Å, $n=13.0$, $l=0.24$ Å.

The 1st coordination sphere is thus independent of concentration. The 2nd coordination sphere is more complex and is less resolved in the more concentrated solution, where the number of water molecules is no longer sufficient to fill out a 2nd coordination sphere. The shape of the RDF in this region indicates that perchlorate groups are bonded in outer-sphere complexes apparently with an orientation corresponding approximately to that of a bidentate ligand.

Similar results are obtained for chloride solutions (Fig. 5) where the complications of a polyatomic counter ion are not present. For 1 M solutions the 1st coordination sphere can be described with the same parameter values as for the perchlorate solution, but the 2nd coordination sphere is slightly changed. Apparently only solvent molecules fill out these positions. In the concentrated solution the 1st coordination peak is still unchanged, but the 2nd sphere is now represented by a double peak, presumably because not only water molecules but also Cl^- ions are present and outer-sphere chloride complexes are formed.

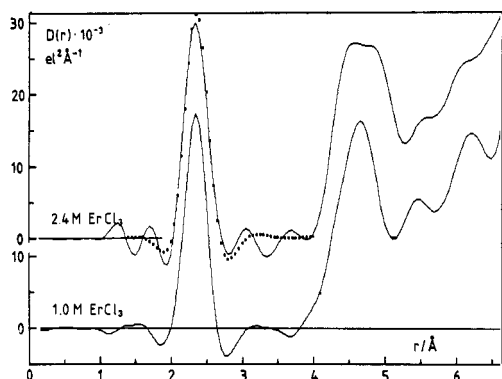


Fig. 5. $D^M(r)$ functions for a 2.40 M (upper curve) and a 1.00 M (lower curve) erbium chloride solution. Both sets normalized to a unit volume containing one Er. The dotted peak is calculated for $\text{Er-H}_2\text{O}$ with $d=2.35$ Å, $n=7.8$, $l=0.09$ Å

The concentrated solutions lead to orientation effects which cannot be easily included in a complete model for the structure and which are not present in the more dilute solutions, where ions are separated by layers of water molecules. In the concentrated solutions on the other hand the 1st coordination sphere is more dominant and can be more precisely determined. The intramolecular interactions, including those of the 1st coordination sphere can be well reproduced by gaussian peaks, which is not, however, the case for the 2nd coordination sphere or for the non-bonding interactions, where the distribution of distances is no longer gaussian.

It is always possible to resolve an RDF into a number of gaussian peaks, but this may not have any physical, or rather chemical, significance. It can be useful, however, for analysing a partly resolved peak. Results obtained with such a procedure have been reported for a series of concentrated lanthanide chloride solutions (ref. 13). For the 1st coordination sphere of erbium the results do not differ significantly from those obtained here using isomorphous substitution. The high charge of the erbium ion leads to strong bonds to its coordinated water molecules and to well-defined coordination spheres. Several investigations of the calcium ion, which has a size ($\text{Ca-H}_2\text{O} = 2.40$ Å) similar to that of Er^{3+} ($\text{Er-H}_2\text{O} = 2.36$ Å) but a lower charge, have been reported for chloride solutions using X-ray scattering (ref. 14-16), neutron scattering (ref. 17,18) and molecular dynamics methods (ref. 16). Compared to the results obtained here Er^{3+} has a lower rms variation ($l=0.10$ Å) than Ca^{2+} ($l=0.14$ Å) and, apparently, a more pronounced 2nd coordination sphere, as would be expected because of the charge difference. For Ca^{2+} , however, values obtained for the coordination number range from about 5 to about 10.

When water molecules in the 1st coordination sphere are replaced by ligands and inner-sphere complexes are formed the effect on the diffraction curves will be the appearance of new interactions, which may not be resolved from other types of interactions. Diffraction measurements on erbium solutions show inner-sphere complex formation with sulfate and selenate, and with nitrate ions. For a 0.8 M erbium selenate solution this is indicated by a peak at 3.75 Å in $D^M(r)$, which can only correspond to an Er-Se interaction (Fig. 6). With distances of 1.63 Å for Se-O and 2.34 Å for Er-O it corresponds to an Er-O-Se angle of about 140° . The SeO_4^{2-} group thus acts as a monodentate ligand, which is similar to the bonding found in crystal structures. The size of the peak corresponds to about 0.5 $\text{SeO}_4^{2-}/\text{Er}$. The 1st coordination sphere is not affected, except for a slight decrease of about 0.02 Å in the Er-O bond length. The remaining oxygens in the bonded selenate group will contribute to the 2nd coordination sphere, the shape of which differs from those in the other solutions.

In the non-erbium RDF part the intramolecular SeO_4 interactions are closely reproduced by theoretical peaks with Se-O distances the same as found in crystal structures. The Er-Se peak is clearly indicated in the original RDF (Fig. 6b). Subtraction of the part involving erbium (Fig. 6c) shows, however, in addition to Se-O interactions at 1.63 Å and $\text{H}_2\text{O-H}_2\text{O}$ interactions at 2.9 Å, an overlapping peak to be present at about 3.9 Å, probably resulting

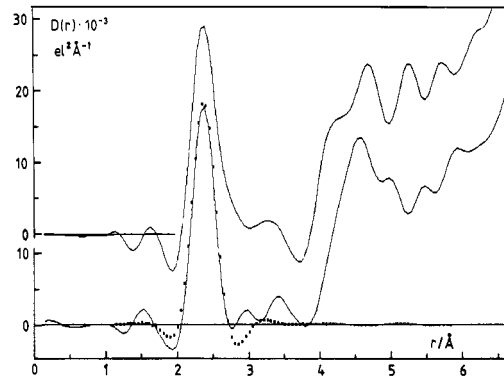
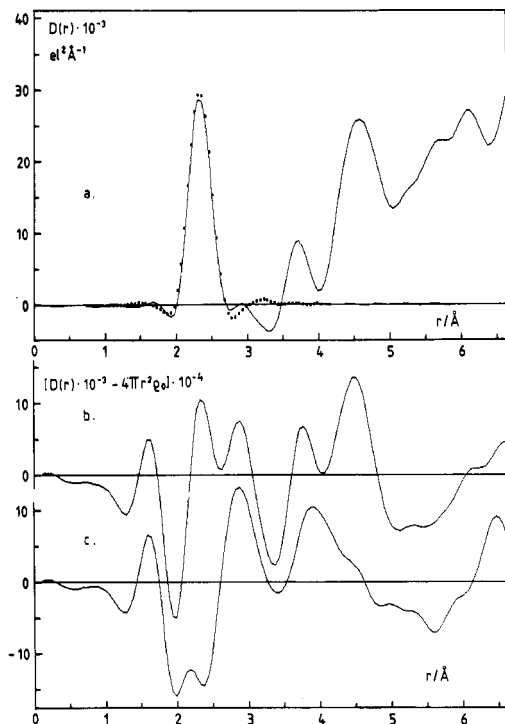


Fig. 7. $D^M(r)$ functions for a 1.00 M erbium nitrate solution with NO_3^- : Er = 3.0 (lower curve) and 9.0 (upper curve). The dotted peak is calculated for Er- H_2O with $d=2.38$ Å, $n=8.0$, $l=0.10$ Å.

Fig. 6. $D^M(r)$ for a 0.8 M $\text{Er}_2(\text{SeO}_4)_3$ solution. Dotted line calculated for Er- H_2O with $d=2.36$ Å, $n=8.0$, $l=0.10$ Å (a). The reduced RDF (b). The reduced RDF with Er interactions subtracted (c).

in part from a hydration sphere around SeO_4^{2-} . This will affect the appearance of the peak in the non-separated RDF, which cannot, therefore, be used for a quantitative analysis, although it shows that a complex formation takes place.

For a 1 M nitrate solution the 1st coordination sphere does not differ from those of the other solutions except for a slightly longer Er- H_2O distance (Fig. 7). An increased concentration of the ligand leads to a broadening of the peak and to the formation of a shoulder at about 4.2 Å on the peak of the 2nd coordination sphere (Fig. 7). A reasonable interpretation is an inner-sphere bonding of one to two nitrate groups as bidentate ligands. The Er-N distance is not resolved from the Er- H_2O distance and the shoulder at 4.2 Å corresponds to the non-bonded oxygen of the nitrate group. As for the selenate complexes the nitrate complex formation is indicated in the original RDF but cannot be separated from overlapping interactions.

INTERPRETATION OF SINGLE DIFFRACTION CURVES

The results indicate that the prospects for investigating weak complex formation and in particular outer-sphere complex formation with diffraction methods are not good unless the resulting peaks occur in a region where they are not distorted by contributions from other types of interactions or a separation of interactions can be made. Obviously, the situation will be more favorable for other types of ligands, preferably containing heavy atoms, and for other types of solvents containing more than one atom that contribute to the scattering. The data analysis then has to be limited to identification and separation of specific intramolecular interactions in the solution. In combination with information from other sources, this can be sufficient for a derivation of the complete structure of the complex. The remaining solution structure cannot be uniquely derived from the diffraction curve but is, on the other hand, not of interest in this context.

An approach (ref. 5,7) that is often used for interpreting solution scattering data, in particular for the determination of hydration numbers of metal ions, involves the construction of a complete model for the solution, including intra- as well as intermolecular interactions, often involving a large number of parameters, which is then refined by a least squares procedure comparing observed and calculated intensity values. For each intramolecular interaction the distance, d , its frequency, n , and its rms variation, l , are used as parameters. The 1st coordination sphere is included for the metal ion and for the counter ion. The water structure is assumed to be that of pure water or is introduced in the refinement as water-water interactions. A 2nd coordination sphere is often included. Beyond the discrete interactions in this "first neighbor model" the structure is approximated by an evenly distributed electron density outside a sphere of a radius R surrounding each atom. A correlation between many of the parameters cannot be avoided but the refinements usually lead to good agreement between observed and calculated values over the whole s range and also lead to realistic values for the hydration numbers. The uncertainties in the derived parameter values, however, are difficult to estimate, but are likely to be much larger than the standard deviations seem to indicate. The results discussed for the erbium

solutions show that distances within a 2nd coordination sphere and between water molecules in the water structure and other intermolecular interactions cannot be described by gaussian distributions and they are not usually resolved from other interactions. The same may be true for the 1st coordination sphere, if the bonds to the metal ions are weak. The emergence of a continuum of electron density outside a sphere surrounding an atom is a convenient but simplified description. Because many of the parameters are not independent, the choice of model may affect the results obtained. Taking the erbium nitrate complexes as an example, the metal-nitrogen interactions would be dependent on assumptions made about the H₂O-H₂O interactions. For the selenate complexes the metal-selenium interactions would be affected by assumptions made about intermolecular interactions.

Monoatomic ligands

The major part of the investigations of complex formation by diffraction methods, reported in the literature, involves monoatomic ligands, primarily halide ions. Metal-chloride distances in an inner-sphere complex will usually appear in a region between the metal-oxygen bonding distances and the H₂O-H₂O distances of the bulk water and will, at least in part, be resolved in the RDFs. Inner-sphere complex formation with chloride can then be easily distinguished, the metal chloride bonding distance can be precisely determined, and the number of metal-chloride bonds per metal ion can be approximately estimated. For the heavier halide ions, bromide and iodide, the metal-ligand and ligand-ligand distances will be longer, but the corresponding interactions will be more dominant because of the higher atomic numbers, and therefore, more easily distinguished in the distribution functions.

For a determination of the coordination geometry of a complex the metal halide distance and frequency are not sufficient. The ligand-ligand interactions are also needed, but cannot usually be determined because of overlapping intermolecular interactions. As a further complication several different complexes are usually present simultaneously in a solution. An analysis, based on a single diffraction curve, will then give an average over the different complexes, and the coordination geometry, which may be different for the different complexes, cannot be determined. Detailed information on the structures can only be obtained by measuring diffraction curves over a range of ligand and metal ion concentrations for solutions in which the concentrations of the individual complexes are known. Only very few determinations of this kind have been carried out.

In an investigation (ref. 19,20) of the halide complexes of the thallium(III) ion, the stability constants for the concentrated solutions needed for the diffraction measurements were determined from NMR measurements of thallium-205 chemical shifts. Solutions with known concentrations of the different complexes, which have well separated regions of existence, could then be prepared. From the corresponding diffraction curves the Tl-X and the X-X interactions could be analyzed and a unique structure could be derived for each complex (Fig. 8). The water positions within the complexes could not, however, be determined, with exception for the hydrated Tl³⁺ ion, Tl(H₂O)₆³⁺, since the corresponding Tl-H₂O interactions could not be separated from other interactions in the diffraction curves. Knowing the positions of Tl and X, likely positions for the water molecules could be deduced using information from related crystal structures. The contribution from the complexes dominates the scattering curves and the remaining structure in the solution, which cannot be determined, does not affect the results of the analysis. The hydrated thallium(III) ion is octahedrally coordinated with six equidistant water molecules. The TlX₂⁺ ion is linear, but four H₂O are probably weakly coordinated leading to an approximately octahedral arrangement. The bonding of a third X⁻ ion results in a planar trigonal complex. The fourth X⁻ ion gives a regular tetrahedral TlX₄⁻ complex. In chloride solutions an octahedral TlCl₆³⁻ complex is formed at high Cl/Tl ratios. The coordination changes are accompanied by a continuous increase in the Tl-X bond length (Fig. 8).

The halide complexes formed by zinc in aqueous solution (ref. 21) are less favorable for a diffraction investigation since the regions of existence of the different complexes overlap and solutions containing only one dominant complex cannot be prepared. The relative concentrations for the different complexes can, however, be determined from the Raman spectra of the solutions and with the use of this information the diffraction curves lead to structure determinations of the different complexes.

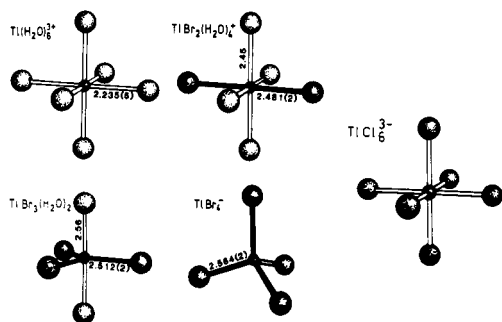


Fig. 8. Structures derived from diffraction data for thallium halide complexes in aqueous solution.

Similar structure derivations have been done for the mercury(II) halide complexes in aqueous solutions (ref. 22,23) and in non-aqueous solvents (ref. 24-26). In the aprotic solvent DMSO mercury(II) forms similar halide complexes as in aqueous solution, all with a high solubility and with well separated regions of stability. DMSO coordinated to Hg^{2+} will give contributions to the diffraction curve not only from Hg-O but also from Hg-S and Hg-C interactions. Since these interactions can be identified from the diffraction curves the orientation of the coordinated DMSO molecule can be determined. The solvated Hg^{2+} ion in DMSO is octahedrally coordinated, the bonding being via oxygen with an Hg-O-S angle of 120° (ref. 27), which does not differ significantly from the value found in the crystalline solvate. This octahedral coordination changes into an approximately linear coordination in HgX_2 . The I-Hg-I angle in HgI_2 is determined to be 159° and two weakly coordinated DMSO molecules can be distinguished from the Hg-S interactions. The HgI_3^- complex forms a slightly flattened tetrahedron with a DMSO probably occupying the fourth tetrahedral site. The HgBr_3^- and the HgCl_3^- complexes are closer to a planar trigonal structure with two coordinated DMSO molecules above and below the plane. The HgX_4^{2-} complexes are regular tetrahedra.

Other non-aqueous solvents have similar advantages. The structure of the HgX_2 complexes have been investigated also in methanol (ref. 25), pyridine (ref. 28,29) and tetrahydrothiophene (ref. 30). The X-Hg-X angle has been found to vary with the solvent and the results have made it possible to correlate the structural changes in the HgX_2 complex with the donor properties of the solvent.

Polyatomic ligands

Only a limited number of diffraction measurements on complexes containing polyatomic ligands have been reported in the literature. Investigations of zinc sulfate solutions indicate that the method of refining a complete model for the solution using a single diffraction curve is too insensitive to prove the presence or non-presence of this type of complex formation (ref. 31-33). For a unique identification of metal-sulfur interactions comparisons between diffraction curves for solutions of different concentrations are needed.

For erbium selenate solutions the Er-O-Se angle was found to be 140° , which shows the SeO_4^{2-} group to be bonded as a monodentate ligand (ref. 12). In cadmium sulfate solutions the Cd-O-S angle has been found to be 134° , which is similar to values found in crystal structures (ref. 34-36). Similar M-O-S angles have been reported for sulfate complexes of other metal ions: Cr^{3+} (ref. 37), Fe^{3+} (ref. 38), In^{3+} (ref. 39), Ni^{2+} (ref. 40), Mn^{2+} (ref. 40,41).

In nitrate complexes of Ag^+ in aqueous solutions and in molten salts the NO_3^- ion is monodentate with an Ag-O-N angle of about 115° (ref. 42,43) and the same type of bonding has been found for Cd^{2+} (ref. 44) and Mn^{2+} (ref. 45). Structures of phosphate complexes with Ni^{2+} and Ca^{2+} (ref 46) and oxalate complexes with Fe^{3+} (ref. 47) have been derived. Transition metal complexes with several organic ligands have been investigated by Ohtaki and coworkers (ref. 48,49).

Tetrathiocyanate, SCN^- , is an ambidentate ligand with three atoms contributing to the scattering. Its configuration in a metal ion complex can therefore be determined and structures of complexes with mercury(II), cadmium(II) and zinc(II) ions have been investigated in aqueous (ref. 50) and DMSO (ref. 51) solutions.

Polynuclear complexes

A group of complexes, which can be profitably studied by diffraction methods, are polynuclear complexes and cluster compounds. In the presence of heavy metal atoms the metal-metal interactions within the complexes will give distinct contributions to the scattering curves and the radial distribution functions, and precise parameters for the interactions can be determined. The metal-metal distances give information on the type of bridging between the metal atoms in the complexes and the number of interactions per metal atom shows the degree of condensation. With the compositions of the complexes known from equilibrium data and with use of information from crystal structures on the bonding characteristics of the particular metal ion, the structure can often be derived.

Several polynuclear hydrolysis complexes of metal ions have been investigated in this way. When a hydrated metal ion dissociates its protons the mononuclear hydroxo complexes first formed are often condensed into larger complexes in which the metal ions are joined by bridging hydroxo or oxo groups. This is not usually a process of a continuous building up of larger and larger complexes before the ultimate precipitation of hydroxide or oxide. Most metal ions seem to form a limited number of discrete well-defined complexes, each dominant within a particular pH interval. The compositions of the complexes and their stability constants can be determined from equilibrium measurements. From diffraction curves on solutions containing an optimal amount of a particular complex, as estimated from the stability constants, the metal-metal interactions can be analyzed. Structures have been derived for hydrolysis complexes of Pb^{2+} (ref. 52), Bi^{3+} (ref. 53,54), Hg^{2+} (ref. 55), Sn^{2+} (ref. 56), Th^{4+} (ref. 57,58), U^{4+} (ref. 59), UO_2^{2+} (ref. 60), Zr^{4+} and Hf^{4+} (ref. 61), In^{3+} (ref. 62).

The radial distribution function for a non-hydrolyzed slightly acid indium nitrate solution is compared in Fig. 9 with that for a hydrolyzed solution of the same concentration with a

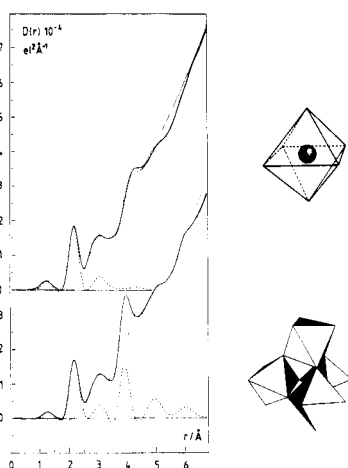


Fig. 9. Radial distribution functions for a slightly acid 4.0 M indium nitrate solution (upper curve) and a hydrolyzed solution (lower curve) both normalized to a unit volume containing one In atom. Dashed lines are theoretical curves for $\text{In}(\text{H}_2\text{O})_6^{3+}$ (upper) and $\text{In}_4(\text{OH})_4(\text{H}_2\text{O})_{12}^{8+}$ (lower) assumed to be present in the solutions.

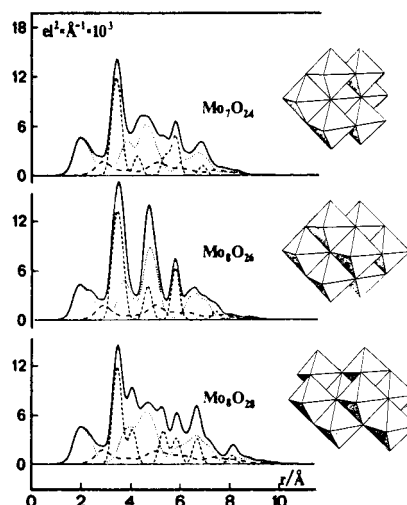


Fig. 10. Calculated peak shapes for some structurally related isopoly-molybdate ions (solid lines). The separate contributions from Mo-Mo (short dashes), Mo-O (dots) and O-O (long dashes) interactions are shown.

composition corresponding to a removal of 0.75 protons per hydrated indium ion (ref. 62). The difference between the two curves shows a sharp peak at 3.89 Å. In crystal structures this is the distance found between two In atoms joined by a single hydroxo bridge. The peak at 2.17 Å is the same in both solutions and corresponds to the 1st coordination sphere of the In^{3+} ion. It is consistent with an octahedral coordination. The hydrolysis complexes are thus built up from InO_6 octahedra sharing corners. An analysis of the peak shape, the absence of other In-In peaks and results of equilibrium measurements leads to a structure containing four tetrahedrally arranged In atoms. Calculated structure factors and peak shapes for this complex are in agreement with the diffraction curve.

The structures of more complex species may not be possible to determine, but diffraction curves can be used for their identification, if similar complexes are known from crystal structure determinations. Structural changes in the complexes with changing compositions of the solutions can then be followed and analyzed with the use of diffraction curves. The heptamolybdate ion $\text{Mo}_7\text{O}_{24}^{6-}$ is well known from crystal structure determinations. It occurs as the dominant complex in solutions obtained by acidification of a Na_2MoO_4 solution. On further acidification it changes its structure and is partially converted into another poly-molybdate ion. This process and the structural changes that take place can be followed by diffraction measurements.

Calculated contributions from some known isopoly-molybdate ions to a radial distribution curve are shown in Fig. 10. Although they are structurally closely related the calculated peak shapes are characteristically different. The Mo-Mo interactions give the pronounced features to the shape of the curve, while oxygen-oxygen contributions, although larger numerically, give a more diffuse background curve (Fig. 10). For the heptamolybdate the same features can be recognized in the experimental data for a heptamolybdate solution. On further acidifying this solution the corresponding distribution functions show characteristic changes which can be used to identify the new complex formed, which is an octamolybdate, $\text{Mo}_8\text{O}_{26}^{4-}$ (ref. 63).

SUMMARY

X-ray diffraction investigations on solutions can often give a unique structural information on dissolved complexes, which cannot be directly obtained by other methods. For selected systems with complexes that dominate the scattering or where separation of interactions can be made, for example by isomorphous substitution, a complete and precise structure determination can be made. For other systems the information will be limited because intramolecular interactions of interest cannot be resolved from other types of interactions. These difficulties are of a principal nature and cannot be overcome by sophisticated data handling procedures. Diffraction measurements on a series of solutions in which the concentration of a specific species is systematically varied, is needed in order to get an optimal information on the structures.

Acknowledgements Support of the research program from the Swedish Natural Science Research Council (NFR) and from the foundation "Knut and Alice Wallenbergs Stiftelse" is gratefully acknowledged. I thank Dr. M. Sandström for discussions and E. Hansen and I. Desselberger for technical assistance.

REFERENCES

1. K.F. Ludwig Jr, W.K. Warburton and A. Fontaine, *J. Chem. Phys.* **87**, 620 (1987).
2. K.F. Ludwig Jr, W.K. Warburton, L. Wilson and A.I. Bienenstock, *J. Chem. Phys.* **87**, 604 (1987).
3. A.K. Soper, G.W. Neilson, J.E. Enderby and R.A. Howe, *J. Phys.* **C10**, 1793 (1977).
4. W. Bol, G.J.H. Gerrits and C.L.vP Eck, *J. Appl. Crystallogr.* **3**, 486 (1970).
5. G. Pálincás and E. Kálmán, in "Diffraction Studies on non-Crystalline Substances" (ed. I. Hargittai and W.J. Orville-Thomas), Elsevier 1981.
6. H. Ohtaki, *Revs. Inorg. Chem.* **4**, 103 (1982).
7. R. Caminiti, G. Licheri, G. Piccaluga, G. Pinna and M. Magini, *Revs. Inorg. Chem.* **1**, 333 (1979).
8. J.E. Enderby and G.W. Neilson in "Water a Comprehensive Treatise", (ed. F. Franks) Plenum Press.
9. G.W. Neilson and J.E. Enderby, *Ann. Rep. Progr. Chem.*, **C76**, 185 (1979).
10. J.E. Enderby, S. Cummings, G.J. Herdman, G.W. Neilson, P.S. Salmon and N. Skipper, *J. Phys. Chem.* **91**, 5851 (1987).
11. G. Johansson and R. Caminiti, to be published.
12. G. Johansson and H. Wakita, *Inorg. Chem.* **24**, 3047 (1985).
13. A. Habenschuss and F.H. Spedding, *J. Chem. Phys.* **73**, 444 (1980).
14. J. N. Albright, *J. Chem. Phys.* **56**, 3783 (1972).
15. G. Licheri, G. Piccaluga and G. Pinna, *J. Chem. Phys.* **64**, 2437 (1976).
16. M.M. Probst, T. Radnai, K. Heinzinger, P. Bopp and B.M. Rode, *J. Phys. Chem.* **89**, 753 (1985).
17. S. Cummings, J.E. Enderby and R.A. Howe, *J. Phys. C: Solid State Phys.* **13**, 1 (1980).
18. N.A. Hewish, G.N. Neilson and J.E. Enderby, *Nature* (London) **297**, 138 (1982).
19. J. Glaser and G. Johansson, *Acta Chem. Scand.* **A36**, 125 (1982).
20. J. Glaser, *Acta Chem. Scand.* **A36**, 451 (1982).
21. P. Goggin, G. Johansson, M. Maeda and H. Wakita, *Acta Chem. Scand.* **A38**, 625 (1984).
22. M. Sandström and G. Johansson, *Acta Chem. Scand.* **A31**, 132 (1977).
23. M. Sandström, *Acta Chem. Scand.* **A31**, 141 (1977).
24. F. Gaizer and G. Johansson, *Acta Chem. Scand.* **22**, 3013 (1968).
25. M. Sandström, *Acta Chem. Scand.* **A32**, 627 (1978).
26. S. Ahrland, E. Hansson, Å. Iverfeldt, and I. Persson, *Acta Chem. Scand.* **A35**, 275 (1981).
27. M. Sandström, I. Persson and S. Ahrland, *Acta Chem. Scand.* **A32**, 607 (1978).
28. I. Persson, M. Sandström, P. Goggin and A. Mosset, *J. Chem. Soc. Dalton Trans.* 1597 (1985).
29. Å. Iverfeldt and I. Persson, *Inorg. Chim. Acta* **111**, 171 (1986).
30. M. Sandström, I. Persson and P. Goggin, *J. Chem. Soc. Dalton Trans.* 2411 (1987).
31. G. Licheri, G. Paschina, G. Piccaluga and G. Pinna, *Z. Naturforsch.* **37a**, 1205 (1982).
32. T. Radnai, G. Pálincás and R. Caminiti, *Z. Naturforsch.* **37a**, 1247 (1982).
33. A. Musina, G. Paschina, G. Piccaluga and M. Magini, *J. Appl. Cryst.* **15**, 621 (1982).
34. R. Caminiti and G. Johansson, *Acta Chem. Scand.* **A35**, 451 (1981).
35. R. Caminiti and G. Johansson, *Acta Chem. Scand.* **A35**, 373 (1981).
36. R. Caminiti, *Z. Naturforsch.* **36a**, 1062 (1981).
37. R. Caminiti, *Chem. Phys. Lett.* **86**, 214 (1982).
38. M. Magini, *J. Chem. Phys.* **70**, 317 (1979).
39. R. Caminiti and G. Paschina, *Chem. Phys. Lett.* **82**, 487 (1981).
40. G. Licheri, G. Paschina, G. Piccaluga and G. Pinna, *J. Chem. Phys.* **81**, 6059 (1984).
41. R. Caminiti, G. Marongiu and G. Paschina, *Z. Naturforsch.* **37a**, 581 (1982).
42. T. Yamaguchi, G. Johansson, B. Holmberg, M. Maeda and H. Ohtaki, *Acta Chem. Scand.* **A38**, 437 (1984).
43. B. Holmberg and G. Johansson, *Acta Chem. Scand.* **A37**, 367 (1983).
44. R. Caminiti, P. Cucca and T. Radnai, *J. Phys. Chem.* **88**, 2382 (1984).
45. R. Caminiti, P. Cucca and T. Pintori, *Chemical Phys.* **88**, 155 (1984).
46. R. Caminiti, *J. Chem. Phys.* **77**, 5682 (1982).
47. M. Magini, *Chem. Phys. Lett.* **78**, 106 (1981).
48. S.-I. Ishiguro and H. Ohtaki, *J. Coord. Chem.* **15**, 237 (1987).
49. H. Ohtaki, *Revs. Inorg. Chem.* **4**, 103 (1982).
50. I. Persson, Å. Iverfeldt and S. Ahrland, *Acta Chem. Scand.* **A35**, 295 (1981).
51. H. Ohtaki, *Pure and Appl. Chem.* **59**, 1143 (1987).
52. G. Johansson and Å. Olin, *Acta Chem. Scand.* **22**, 3197 (1968).
53. H. A. Levy, M. D. Danford and P. A. Agron, *J. Chem. Phys.* **31**, 1458 (1959).
54. B. Sundvall, *Acta Chem. Scand.* **A34**, 93 (1980).
55. G. Johansson, *Acta Chem. Scand.* **25**, 2799 (1971).
56. G. Johansson, and H. Ohtaki, *Acta Chem. Scand.* **27**, 643 (1973).
57. G. Johansson, *Acta Chem. Scand.* **22**, 399 (1968).
58. M. Magini, A. Cabrini, G. Scibona, G. Johansson and M. Sandström, *Acta Chem. Scand.* **A30**, 437 (1976).
59. S. Pocev and G. Johansson, *Acta Chem. Scand.* **27**, 2146 (1973).
60. M. Åberg, *Acta Chem. Scand.* **24**, 2901 (1970).
61. M. Åberg, *Acta Chem. Scand.* **B31**, 171 (1977).
62. R. Caminiti, G. Johansson and I. Toth, *Acta Chem. Scand.* **A40**, 435 (1986).
63. G. Johansson, L. Pettersson and N. Ingri, *Acta Chem. Scand.* **A33**, 305 (1979).